Analysis of the atomic fine structure, using a nonrelativistic many-body and a relativistic central-field approach

Ingvar Lindgren and Ann-Marie Mårtensson
Department of Physics, Chalmers University of Technology, Göteborg, Sweden
(Received 16 June 1981)

Nonrelativistic many-body calculations of the fine structure of *nd* states of sodiumlike systems have been performed for $Z=11-42$, taking into account the core polarization to first order in the spin-orbit coupling and to all orders in the Coulomb interaction. The results agree well with the experimental data available, and, in particular, the transition from inverted- to normal-level ordering appears at the right place, around $Z=15$. The alternative approach of evaluating the fine structure by means of relativistic central-field calculations—introduced by Luc-Koenig—is analyzed in detail, using the Pauli approximation and a graphical form of perturbation theory. Provided the self-consistent Hartree-Fock potential is used for the core, it can be shown that the relativistic method is (to order α^2) equivalent to a nonrelativistic calculation, where the core polarization is included to all orders of the Coulomb interaction. In the calculation of Luc-Koenig a local core potential is used, in which case this equivalence is only partial. In order to be able to make accurate comparisons with our many-body results, we have performed relativistic calculations using the full Hartree-Fock potential of the core.

I. INTRODUCTION

It is well known that many alkali-metal states exhibit an anomalous fine structure. The *nd* states of sodium and the *nf* states of cesium, for instance, have an inverted fine structure[1]—with the higher j state lower in energy—in contrast to the predictions of any nonrelativistic central-field model (CFM).

In order to calculate the fine-structure splitting beyond the nonrelativistic CFM essentially two approaches are available. In one approach, which has been used by several groups,[2–5] the "Pauli operators"—i.e., the spin-orbit interaction and the other operators emanating from the reduction of the relativistic many-body equation to its Pauli limit—are used as a perturbation in a nonrelativistic perturbation expansion or configuration-interaction calculation. In the other approach, introduced by Luc-Koenig,[6,7] the Dirac equation is solved for the valence electron in the relativistic potential of the core. The fine-structure separation then appears directly as the eigenvalue difference for the two states. It has been found that the two approaches yield essentially the same numerical results, and it is the main purpose of the present work to investigate their equivalence in detail.

There has been some concern lately that, in spite of its successes in reproducing experimental results, the relativistic Hartree-Fock (HF) approach may lack a sound foundation. The many-electron Hamiltonian, which is used to obtain the HF equation, has, in fact, no bound solutions.[8,9] It has been pointed out by Sucher[9] that it is not clear to what Hamiltonian the HF equation is an approximation and the use of projection operators for positive energy states has been advocated.[8,9] This leads to rather complicated equations. However, in a recent article Mittlemann[10] has shown that, provided that the projection operator is expressed in terms of eigenfunctions to the HF equation, the HF approximation of the projected Hamiltonian leads to the same single-electron eigenvalues as the HF approximation of the unprojected Hamiltonian. We will not here consider this problem any further. Our main purpose is to compare two commonly used methods for actual calculations.

The relation between the relativistic central-field and the nonrelativistic many-body approaches was first discussed by Luc-Koenig,[6] considering the perturbations of the orbitals caused by the Pauli operators. In that paper, however, Luc-Koenig considers only the effect of the perturbation on the *valence* orbital and interprets the anomalous fine structure as due to the relativistic shift of that orbital. In the present paper we shall show that such

a shift has only a minor effect on the fine structure and cannot cause any inversion. Instead, it is found that the main reason for the anomalous fine structure is the relativistic shifts of the *core* orbitals, which cause the exchange potential for the valence electron to be j dependent. This effect is present also if the radial distribution of the valence electron is the same for the two j states. This interpretation agrees with that given by Luc-Koenig in a later paper.[7] This interpretation was given also by Pyper and Marketos[11] in a recent paper, in which they performed relativistic calculations of the fine structure for a number of d and f states and explicitly calculated the contribution from the valence electrons and from the exchange interaction with the core. They used relativistic Hartree-Fock orbitals for the core but a hydrogenlike function for the valence electron in order to circumvent numerical difficulties in obtaining the valence contribution. However, as we shall see, the hydrogenic orbitals, although giving a qualitatively correct description, underestimates the influence of the core-valence exchange interaction.

In the calculation of Luc-Koenig[6,7] the core orbitals are generated in a *local* potential, which means that the exchange interaction between the core electrons is not taken into account in a self-consistent way. Such a calculation is essentially equivalent to a nonrelativistic calculation, where the core polarization is included to first order in the spin-orbit interaction as well as in the Coulomb interaction. It will be shown in the present paper, however, that when the self-consistent Hartree-Fock potential of the core is used, the relativistic procedure is—to order α^2 (α being the fine-structure constant)—equivalent to a nonrelativistic many-body calculation, where the core polarization is included to first order in the spin-orbit interaction and to *all* orders in the Coulomb interaction. Therefore, in order to be able to make accurate comparisons with our many-body results, we have performed calculations similar to those of Luc-Koenig, using the full Hartree-Fock potential of the core.

We shall begin this paper with a short description of the nonrelativistic many-body and the relativistic Hartree-Fock procedures. In the description of the many-body approach we shall introduce a graphical representation, which we shall use later in comparing the two approaches. This comparison will be based on the Pauli approximation, where the relativistic equations are reduced to equivalent equations (to order α^2) for the large components only. By means of a graphical expansion of the large component in terms of nonrelativistic perturbations, it will then be easy to demonstrate the degree of equivalence of the two approaches. Finally, we shall in this paper as illustrations present some numerical results using the nonrelativistic many-body as well as the relativistic Hartree-Fock procedures.

II. THE NONRELATIVISTIC MANY-BODY APPROACH

The normal starting point for nonrelativistic many-body calculations is the Schrödinger Hamiltonian

$$H_S=\sum_{i=1}^{N} h_S(i)+\sum_{i<j=1}^{N}\frac{1}{r_{ij}}\,, \tag{1}$$

where

$$h_S(1)=-\tfrac{1}{2}\vec{\nabla}_1^2-\frac{Z}{r_1} \tag{2}$$

is the Schrödinger Hamiltonian for a single electron moving in the nuclear field. The second term in (1) represents the electron-electron repulsion in the nonrelativistic limit.

In the central-field approximation the Hamiltonian (1) is replaced by a central-field (CF) Hamiltonian

$$H_S^{\mathrm{CF}}=\sum_{i=1}^{N} h_S^{\mathrm{CF}}(i)\,, \tag{3}$$

where

$$h_S^{\mathrm{CF}}(1)=-\tfrac{1}{2}\vec{\nabla}_1-\frac{Z}{r_1}+U_S(r_1) \tag{4}$$

is the Hamiltonian for an electron moving in the field of the nucleus and an average, central field due to the other electrons. The difference between the operators (1) and (3)

$$H_S^{\mathrm{NC}}=-\sum_i U_S(r_i)+\sum_{i<j}\frac{1}{r_{ij}} \tag{5}$$

which is essentially the noncentral (NC) part of the electron-electron interaction, is then treated as a perturbation.

In the following we shall restrict ourselves to alkali-metal-like systems with a single valence electron outside a core of filled shells. As in our work on the hyperfine structure of alkali-metal atoms,[12,13] the central potential used is the

Hartree-Fock potential of the electron core, here denoted by U_S^{HF}. (The neglect of the valence electron in the potential is compensated for by certain higher-order terms in the perturbation expansion.) An arbitrary matrix element of this potential is

$$\langle i \mid U_S^{\mathrm{HF}} \mid j \rangle = \sum_a^{\mathrm{core}} \left[\left\langle ia \left| \frac{1}{r_{12}} \right| ja \right\rangle - \left\langle ia \left| \frac{1}{r_{12}} \right| aj \right\rangle \right], \tag{6}$$

where $|i\rangle$ and $|j\rangle$ represent nonrelativistic Hartree-Fock orbitals, i.e., eigenfunctions of the single-electron Hamiltonian (4) with U_S equal to U_S^{HF}. It follows immediately that the corresponding matrix elements of the perturbation (5) vanish, when the Hartree-Fock potential is used. Therefore, with this potential the eigenvalue of the Hamiltonian (4) is exactly equal to the single-electron energy, i.e., the negative of the electron binding energy, which is Koopmans's theorem.[14]

The Hartree-Fock potential, defined in (6), may also be expressed in the following way:

$$U_S^{\mathrm{HF}}(1) = \sum_a^{\mathrm{core}} \left[a \left| \frac{1}{r_{12}} (1 - P_{12}) \right| a \right]_2, \tag{7}$$

where P_{12} is the exchange operator, which exchanges the coordinates of electrons 1 and 2. The potential is supposed to operate on a function of the coordinates of electron 1, and there is an integration over the coordinates of electron 2. Using this potential in the central-field operator (4), we get the *nonrelativistic Hartree-Fock* (NRHF) operator

$$h_S^{\mathrm{HF}}(1) = h_S(1) + U_S^{\mathrm{HF}}(1) = h_S(1) + \sum_a^{\mathrm{cores}} \left[a \left| \frac{1}{r_{12}} (1 - P_{12}) \right| a \right]_2 . \tag{8}$$

Using the Goldstone-type of diagrams,[15–17] we can represent the matrix elements of the Hartree-Fock potential (6) as shown in Fig. 1. Here the solid lines represent electron orbitals and the dotted lines the Coulomb interaction between the electrons. A summation over the internal lines is assumed. Diagram (a) represents the direct part and diagram (b) the exchange part of this interaction. The corresponding graphical representation of the Hartree-Fock operator (8) is shown in Fig. 2.

In order to calculate the fine-structure splitting, it is necessary to take relativity into account. For this purpose our starting point will be the Dirac-

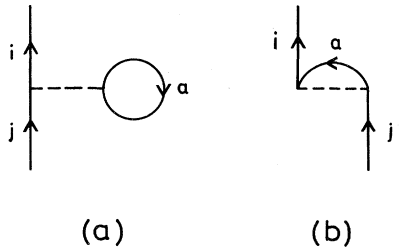

FIG. 1. Goldstone representation of the matrix elements (6) of the nonrelativistic Hartree-Fock potential.

Breit (DB) Hamiltonian[18–20]

$$H_{\mathrm{DB}} = \sum_{i=1}^{N} h_D(i) + \sum_{i<j=1}^{N} g(i,j), \tag{9}$$

where

$$h_D(1) = c\vec{\alpha}_1 \cdot \vec{p}_1 + mc^2(\beta_1 - 1) - \frac{Z}{r_1} \tag{10}$$

is the Dirac Hamiltonian for an electron moving in the nuclear field—i.e., the relativistic analog to the Schrödinger operator (2)—and g represents the electron-electron interaction in the Breit approximation

$$g(1,2) = \frac{1}{r_{12}} \left[1 - \frac{1}{2} \left[\vec{\alpha}_1 \cdot \vec{\alpha}_2 + \frac{(\vec{\alpha}_1 \cdot \vec{r}_{12})(\vec{\alpha}_2 \cdot \vec{r}_{12})}{r_{12}^2} \right] \right]. \tag{11}$$

The first part of the electron-electron interaction (11) is the instantaneous Coulomb interaction, appearing also in the Schrödinger Hamiltonian (1). The second part—called the Breit interaction—can be interpreted as magnetic interactions between the electrons and as a retardation of the Coulomb interaction.

The Breit interactions, which are of order α^2 (where α is the fine-structure constant) describe incorrectly the negative energy states,[18–20] but can be included in a self-consistent procedure provided

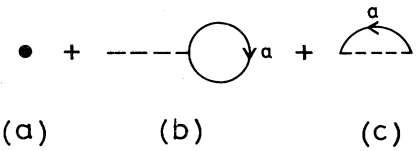

FIG. 2. Graphical representation of the nonrelativistic Hartree-Fock operator (8). The dot represents the Schrödinger operator (2) and the remaining diagrams the Hartree-Fock potential (7).

they are surrounded by projection operators for positive energy states,[9] although this leads to rather complicated equations. Since we are only interested in effects to order α^2, it is sufficient to follow the normal procedure of evaluating the Breit interactions by first-order perturbation theory after a self-consistent solution has been obtained for a Hamiltonian where these interactions have been removed.

In the relativistic formalism the single-electron orbitals are represented by four-component Dirac spinors

$$\Psi=\begin{bmatrix}\psi_1\\ \psi_2\end{bmatrix}, \tag{12}$$

where ψ_1 and ψ_2 are two-component Pauli spinors, referred to as the "large" and the "small" components, respectively. In order to be able to make a comparison with the nonrelativistic treatment, it is convenient to apply the Pauli approximation[18–20] in which the small component of the wave function is eliminated. It can then be shown that the many-body Dirac-Breit Hamiltonian (9) for wave functions composed of four-component Dirac spinors is—to order α^2—equivalent to a "Dirac-Pauli" (DP) operator

$$H_{\rm DP}=H_S+H_P \tag{13}$$

operating on the large components only. Here H_S is the nonrelativistic Hamiltonian (1) and H_P are the so-called Pauli operators. The latter can be decomposed in the following way[18–20]:

$$H_P=H_m+H_D+H_{\rm oo}+H_{\rm so}+H_{\rm ss}\ , \tag{14}$$

where H_m is interpreted as a mass correction, H_D is called the Darwin term (without nonrelativistic analog), and $H_{\rm oo}$, $H_{\rm so}$, and $H_{\rm ss}$ represent the orbit-orbit, spin-orbit, and spin-spin interactions, respectively.

In the nonrelativistic many-body approach we treat the Pauli operators (14) as perturbations—in addition to the noncentral Coulomb interaction (5). This procedure is feasible for light elements, for which αZ is considerably less than unity.

Only the spin-dependent interactions (spin-orbit and spin-spin) can affect the fine structure in the lowest order, i.e., in order α^2. The remaining interactions can affect the fine structure only indirectly, through modifications of the orbitals. This is a second-order effect (of order α^4) and will therefore not be considered in the present analysis. The spin-spin interaction is considerably weaker than the spin-orbit interaction and is usually neglected. In addition, it can be shown that it has no effect on systems with a single valence electron. Therefore, we shall consider only the spin-orbit interaction in the following.

The spin-orbit interaction has the detailed form[18–20]

$$H_{\rm so}=\frac{\alpha^2}{2}\left[\sum_i \frac{Z}{r_i^3}\vec{l}_i\cdot\vec{s}_i-\sum_{i,j}^{i\neq j}\frac{\vec{r}_{ij}\times\vec{p}_i}{r_{ij}^3}(\vec{s}_i+2\vec{s}_j)\right]. \tag{15}$$

This can be interpreted as the interaction between the spin-magnetic moments and the magnetic fields due to the orbital motions of the electrons in the electric field of the nucleus and the other electrons. It can be separated in a "spin-own-orbit" (swo) interaction, involving the interaction between the spin and orbital motions of the *same* electron,

$$H_{\rm swo}=\frac{\alpha^2}{2}\left[\sum_i \frac{Z_i}{r_i^3}\vec{l}_i\cdot\vec{s}_i-\sum_{i,j}^{i\neq j}\frac{\vec{r}_{ij}\times\vec{p}_i}{r_{ij}^3}\cdot\vec{s}_i\right] \tag{16}$$

and a "spin-other-orbit" (soo) interaction, involving the interaction between the spin of one electron and the orbital motions of the other electrons,

$$H_{\rm soo}=-\alpha^2\sum_{i,j}^{i\neq j}\frac{\vec{r}_{ij}\times\vec{p}_i}{r_{ij}^3}\cdot\vec{s}_j\ . \tag{17}$$

The spin-own-orbit interaction—as well as the mass-correction and Darwin terms—originate from the Dirac Hamiltonian (9), while the orbit-orbit, spin-other-orbit, and spin-spin interactions have their origin in the Breit interactions (11).

The spin-orbit interaction (15) can be written as

$$H_{\rm so}=\sum_i V_i+\sum_{i<j}(V_{ij}+V_{ji})\ , \tag{18}$$

where V_i represents the one-body operator

$$V_i=\frac{\alpha^2}{2}\frac{Z}{r_i^3}\vec{l}_i\cdot\vec{s}_i \tag{19}$$

and V_{ij} the two-body operator

$$V_{ij}=-\frac{\alpha^2}{2}\frac{\vec{r}_{ij}\times\vec{p}_i}{r_{ij}^3}\cdot(\vec{s}_i+2\vec{s}_j)\ . \tag{20}$$

Note that we sum here only over distinct electron pairs in order to make the operator more analogous to the Coulomb interaction. Owing to the asymmetry of the two-body spin-orbit interaction, we then have to include V_{ij} as well as V_{ji}.

For numerical work it is convenient to transform the spin-orbit operator to tensor form. This was first done by Blume and Watson,[21] and

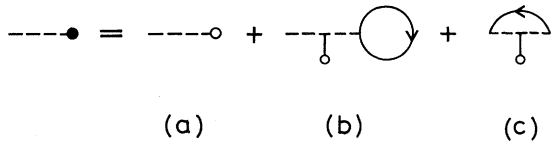

FIG. 3. Graphical representation of the effective spin-orbit interaction (23). Diagram (a) represents the nuclear term (19) and diagrams (b) and (c) the direct and exchange parts, respectively, of the two-body operator (20).

equivalent expressions have been given in later works.[4,5,22] The expression we use, which is taken from the work of Mårtensson,[5] is given in the Appendix.

The one-body part as well as most of the two-body part of the spin-orbit interaction (18) can be included in an *effective* one-body interaction

$$H_{\rm so}^{\rm eff}=\sum_i h_{\rm so}^{\rm eff}(i)\ , \tag{21}$$

where $h_{\rm so}^{\rm eff}$ is defined in analogy with the Hartree-Fock potential (6) by means of the matrix elements

$$\langle i\,|\,h_{\rm so}^{\rm eff}\,|\,j\rangle=\langle i\,|\,V_1\,|\,j\rangle + \sum_a^{\rm core}(\langle ia\,|\,V_{12}+V_{21}\,|\,ja\rangle - \langle ia\,|\,V_{12}+V_{21}\,|\,aj\rangle)\ . \tag{22}$$

This operator may also be expressed by means of the exchange operator in analogy with (7) as

$$h_{\rm so}^{\rm eff}(1)=V_1+\sum_a^{\rm core}\langle a\,|\,(V_{12}+V_{21})(1-P_{12})\,|\,a\rangle_2\ . \tag{23}$$

It can be shown that the effective spin-orbit interaction (23) is of the same tensor form as the ordinary spin-orbit interaction (19), and hence the matrix element above can be expressed as

$$\langle i\,|\,h_{\rm so}^{\rm eff}\,|\,j\rangle=\zeta(i,j)\langle i\,|\,\vec{1}\cdot\vec{s}\,|\,j\rangle\ . \tag{24}$$

A complete expression for the parameter $\zeta(i,j)$ is given in the Appendix.

Graphically we represent the effective spin-orbit interaction (23) as shown in Fig. 3. Diagram (a) represents the nuclear one-body term (V_1) and diagrams (b) and (c) represent the direct and exchange parts, respectively, of the contracted two-body term.

In first order the effect of the spin-orbit interaction is given by the expectation value of the operator (15),(18) in the unperturbed state. For a system with a single valence electron this is exactly equal

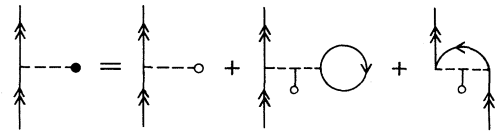

FIG. 4. Graphical representation of the first-order energy contribution (25) due to the effective spin-orbit interaction (23). Double arrows are used to indicate that the orbital line represents the valence orbital.

to the expectation value of the effective operator (23), (24) for the valence electron (m)

$$\Delta E_{\rm so}^{(1)}=\langle m\,|\,h_{\rm so}^{\rm eff}\,|\,m\rangle\ . \tag{25}$$

Using the representation of $H_{\rm so}^{\rm eff}$ given in Fig. 3, we obtain the graphical form of the first-order spin-orbit interaction shown in Fig. 4.

It should be observed that the result above is first order starting from the central-field (Hartree-Fock) model. In order to obtain all contributions of order α^2, we have to combine the spin-orbit perturbation with the Coulomb perturbation (5).

In second order the spin-orbit interaction is combined with *one* interaction of the Coulomb perturbation (5). This leads to the energy contribution

$$\Delta E_{\rm so}^{(2)}=\sum_{a,r}\frac{\langle a\,|\,h_{\rm so}^{\rm eff}\,|\,r\rangle}{\epsilon_a-\epsilon_r}\times\left[\left\langle ma\left|\frac{1}{r_{12}}\right|ra\right\rangle-\left\langle ma\left|\frac{1}{r_{12}}\right|ar\right\rangle\right]+\text{c.c.} \tag{26}$$

Here a runs over all core orbitals and r over all excited (virtual) and valence orbitals, i.e., all orbitals outside the core. The graphical representation of the second-order energy contribution is shown in Fig. 5. Diagrams (a) and (b) represent the terms shown explicitly in (26), diagram (a) with the direct and diagram (b) with the exchange Coulomb interaction. Diagrams (c) and (d) represent the complex conjugate terms, where all matrix elements are

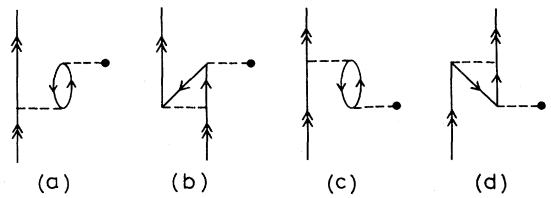

FIG. 5. Graphical representation of the second-order energy contribution due to the combined spin-orbit and Coulomb interactions (26). The interpretation of the diagrams is given in the text.

replaced by their complex conjugates. Since all terms can be assumed to be real, the conjugate terms have the same numerical values as the original ones.

The second-order diagrams in Fig. 5 represent the effect of first-order admixtures into the wave function of states, where a single core orbital has been excited by the Coulomb interaction with the valence electron—or equivalently by the effective spin-orbit interaction. This can be interpreted as a distortion of the core orbitals and is therefore referred to as the *core polarization.*

Owing to the spin dependence of the effective spin-orbit interaction (24), it follows that all diagrams, where this interaction appears on a closed orbital loop, such as the diagrams (a) and (c) in Fig. 5, will vanish.[17] Since then only exchange diagrams contribute, this kind of polarization is also known as the "exchange polarization."

The exchange polarization considered here is quite analogous to that appearing in the hyperfine interaction, which in the case of the quadrupole interaction is commonly known as the "Sternheimer correction."[23] Using the same procedure as in the hyperfine case, Sternheimer and co-workers[2] have calculated the effect of the first-order core polarization—i.e., the second-order energy contribution—on the fine structure and shown that this effect is large enough to explain the inversion observed in some of the alkali-metal sequences. As shown in hyperfine calculations by Garpman *et al.*[12] and by Lindgren *et al.*[13], it is possible to calculate the effect of the core polarization to all orders of perturbation theory—i.e., to all orders of the Coulomb interaction—by solving a system of coupled differential equations in an iterative way. This procedure has been applied also to the fine structure by Holmgren *et al.*[4] and by Mårtensson.[5] In this way all contributions due to single excitations of the core are included. The graphical representation of the fine structure in this approximation is exhibited in Fig. 6. This expansion contains also diagrams with double excitations in intermediate states, such as diagrams (d), (e), (h), and (i). These diagrams appear with all possible orderings between the interactions. It can then be shown that the energy denominators of these diagrams factorize in such a way that the excitations can be treated independently and hence formally as single excitations.[17] The diagrams in Fig. 6 are similar to those appearing in the random-phase approximation (RPA) with exchange, a procedure equivalent to the time-dependent Hartree-Fock (TDHF) procedure.[24]

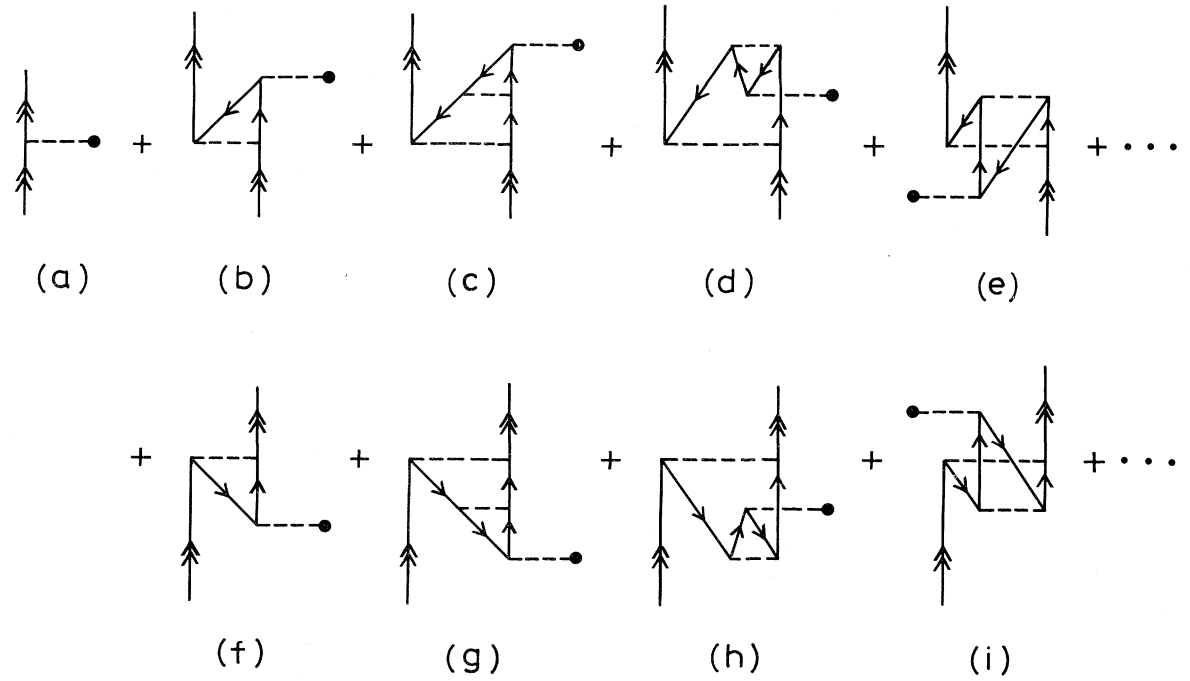

FIG. 6. Graphical representation of the core polarization caused by the first-order spin-orbit interaction in combination with the Coulomb interaction to all orders.

III. THE RELATIVISTIC CENTRAL-FIELD APPROACH

As mentioned previously, the Breit interactions (11), which incorrectly describe interactions involving negative energy states, can be included in a self-consistent procedure of Hartree-Fock type only if projection operators for positive energy states are included,[9] which leads to complicated equations. Therefore, instead of using the Dirac-Breit Hamiltonian (9), it is customary to use the Dirac Hamiltonian

$$H_D=\sum_i h_D(i)+\sum_{i<j}\frac{1}{r_{ij}} \tag{27}$$

as the starting point for the relativistic self-consistent-field procedure.[25,26] In this operator the Breit interactions are removed, and their effect is then—after that self-consistency has been achieved—considered using first-order perturbation theory. This procedure is correct to order α^2.

In the relativistic central-field approximation, the Hamiltonian (27) is further replaced by a central-field Hamiltonian

$$H_D^{\mathrm{CF}}=\sum_i h_D^{\mathrm{CF}}(i)\ , \tag{28}$$

where h_D^{CF} is given by

$$h_D^{\mathrm{CF}}(1)=h_D(1)+U_D(r_1) \tag{29}$$

in complete analogy with the nonrelativistic case (3), (4). The remaining part of the Coulomb interaction

$$H_D^{\mathrm{NC}}=-\sum_i U_D(r_i)+\sum_{i<j}\frac{1}{r_{ij}} \tag{30}$$

which is treated as a perturbation, is identical to the nonrelativistic perturbation (5), apart from any difference in the central potential.

The single-electron orbitals, which are eigenfunctions of the Dirac Hamiltonian (29), are four-component Dirac spinors (12). For a central potential the large and small components can be separated into radial and spin-angular parts as follows[20,25,26]:

$$\begin{aligned}\psi_1&=\frac{1}{r}P_{nlj}(r)\chi_{sljm}(\theta,\phi,\sigma)\ ,\\ \psi_2&=\frac{i}{r}Q_{nlj}(r)\chi_{s\bar{l}jm}(\theta,\phi,\sigma)\ .\end{aligned} \tag{31}$$

Here χ is a vector-coupled spin-angular function and $\bar{l}=2j-l$. This leads to the radial equations

$$\begin{aligned}&\frac{dP}{dr}+\frac{\kappa}{r}P+\left[\frac{2}{\alpha}+\alpha(\epsilon-U_D)\right],\quad Q=0\\ &\frac{dQ}{dr}-\frac{\kappa}{r}Q+\alpha(U_D-\epsilon),\quad P=0\end{aligned} \tag{32}$$

where

$$\kappa=\begin{cases}-(l+1) & \text{for } j=l+\frac{1}{2}\\ 1 & \text{for } j=l-\frac{1}{2}.\end{cases}$$

As before, we shall consider alkali-metal-like systems, and we assume that the potential is the relativistic Hartree-Fock potential from the electron core, which we can express in analogy with the nonrelativistic potential (7) as

$$U_D^{\mathrm{HF}}(1)=\sum_a^{\mathrm{core}}\left[a_D\left|\frac{1}{r_{12}}(1-P_{12})\right|a_D\right]_2\ , \tag{33}$$

where a_D represents a relativistic four-component orbital (Dirac spinor) of the type (12). Inserting this potential in (29), we obtain the *Dirac-Hartree-Fock* (DHF) operator

$$\begin{aligned}h_D^{\mathrm{HF}}(1)&=h_D(1)+U_D^{\mathrm{HF}}(1)\\ &=h_D(1)+\sum_a^{\mathrm{core}}\left[a_D\left|\frac{1}{r_{12}}(1-P_{12})\right|a_D\right]_2 .\end{aligned} \tag{34}$$

In the relativistic Hartree-Fock or Dirac-Hartree-Fock procedure the radial equations (32) are solved self-consistently with the potential (33). Since the valence electron does not appear in the potential we use here, it is sufficient to consider the core electrons in the self-consistent procedure. Then the equations for the valence electron can be solved in the potential of the nucleus and the electron core.

The radial equations (32) depend on the j value of the orbital, and when the Hartree-Fock potential is used the fine-structure splitting for alkali-metal-like systems appears in this procedure directly as an eigenvalue difference for the two orbitals with the same nl quantum numbers according to Koopmans's theorem, mentioned above—apart from the effect of the Breit interaction, which is considered separately, as described previously. For the alkali-metal d states, however, the fine structure is so small—of the order of 10^{-6} a.u. for the sodium sequence—that it is difficult to determine the eigenvalues with sufficient accuracy, when the nonlocal exchange potential is included. For that reason Pyper and Marketos[11] use hydrogenlike

valence orbitals and Luc-Koenig[6] solves the eigenvalue equations for the valence electron in a potential which does not contain the exchange with the core and then treats the exchange interaction using first-order perturbation theory. In a later paper,[7] Luc-Koenig includes also the exchange with the core in the potential for the valence electron. We shall analyze these calculations later, after having established the correspondence between the relativistic central-field and the nonrelativistic many-body approaches.

IV. COMPARISON BETWEEN THE RELATIVISTIC CENTRAL-FIELD AND THE NONRELATIVISTIC MANY-BODY APPROACHES

In order to be able to compare the results of a relativistic central-field calculation with those of the nonrelativistic many-body approach, we shall find a perturbation expansion of the relativistic results based on the Pauli approximation.

As mentioned previously, the Dirac-Breit Hamiltonian (9)—using four-component Dirac spinors to represent the single-electron states—is equivalent to order α^2 to the Dirac-Pauli Hamiltonian (13), when the states are represented by the large components only. In the self-consistent procedure, however, we start from the Dirac Hamiltonian (27), where the Breit interactions are removed. Then it follows that this operator is equivalent to a "reduced" Dirac-Pauli operator

$$H'_{\mathrm{DP}}=H_S+H'_P\ , \tag{35}$$

where

$$H'_P=H_m+H_D+H_{\mathrm{swo}} \tag{36}$$

represents the parts of the Pauli operators (14) which originate from the Dirac equation, namely the mass correction, the Darwin term, and the spin-own-orbit interaction. (The remaining parts originate from the Breit interactions.)

As mentioned before, only the spin-orbit interaction affects the fine structure in order α^2. Therefore, we need here consider only the spin-own-orbit interaction, H_{swo}. In analogy with the complete spin-orbit interaction (18), we write this as

$$H_{\mathrm{swo}}=\sum_i V_i+\sum_{i<j}(V'_{ij}+V'_{ji})\ , \tag{37}$$

where, according to (16), V'_{ij} is given by

$$V'_{ij}=-\frac{\alpha^2}{2}\frac{\vec{\mathrm{r}}_{ij}\times\vec{\mathrm{p}}_i}{r_{ij}^3}\cdot\vec{\mathrm{s}}_i\ . \tag{38}$$

Using the form (1) of the Schrödinger operator

$$H_S=\sum_i h_S(i)+\sum_{i<j}\frac{1}{r_{ij}} \tag{39}$$

and omitting the mass correction and the Darwin term which are j independent, we can express the reduced Dirac-Pauli operator (35) as

$$H'_{\mathrm{DP}}=\sum_i[h_s(i)+V_i]+\sum_{i<j}\left[\frac{1}{r_{ij}}+V'_{ij}+V'_{ji}\right]\ . \tag{40}$$

Within order α^2, this operator has the same eigenvalues, using two-component Pauli spinors, as does the Dirac Hamiltonian

$$H_D=\sum_i h_D(i)+\sum_{i<j}\frac{1}{r_{ij}} \tag{41}$$

when four-component Dirac spinors are used to represent the single-electron states. Thus, in going from the fully relativistic Dirac-Hartree-Fock procedure to the corresponding Pauli scheme based on equations for the large components only, we shall make the following substitutions:

$$\begin{aligned} &h_D(1)\rightarrow h_S(1)+V_1\ ,\\ &\frac{1}{r_{12}}\rightarrow\frac{1}{r_{12}}+V'_{12}+V'_{21}\ . \end{aligned} \tag{42}$$

With these substitutions we obtain the following Pauli analog of the DHF operator (34):

$$h_P^{\mathrm{HF}}(1)=h_S(1)+V_1+\sum_a^{\mathrm{core}}\left[a_P\left|\left[\frac{1}{r_{12}}+V'_{12}+V'_{21}\right](1-P_{12})\right|a_P\right]_2 \tag{43}$$

which we shall refer to as the *Pauli-Hartree-Fock* (PHF) operator. Introducing the PHF potential in analogy with (7) and (33)

$$U_P^{\mathrm{HF}}(1)=\sum_a^{\mathrm{core}}\left[a_P\left|\frac{1}{r_{12}}(1-P_{12})\right|a_P\right]_2 \tag{44}$$

and an effective spin-orbit interaction

$$h'^{\,\mathrm{eff}}_{\mathrm{so}}(1)=V_1+\sum_a^{\mathrm{core}}(a_P\,|\,(V'_{12}+V'_{21})(1-P_{12})\,|\,a_P)_2 \tag{45}$$

in analogy with (23), we may express the PHF operator (43) simply as

$$h_P^{\mathrm{HF}}(1)=h_S(1)+U_P^{\mathrm{HF}}(1)+h'^{\,\mathrm{eff}}_{\mathrm{so}}(1)\ . \tag{46}$$

The graphical representation of the PHF opera-

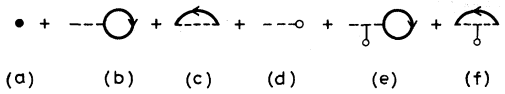

FIG. 7. Graphical representation of the Pauli-Hartree-Fock operator (43),(46). Heavy lines are used to represent the orbitals in the Pauli approximation.

tor (43), (46) is given in Fig. 7, where we use heavy lines to represent the orbitals in the Pauli approximation. Diagram (a) represents the nonrelativistic Schrödinger operator (2) and diagrams (b) and (c) the PHF potential (44). Diagrams (d)–(f) represent the effective spin-orbit interaction (45) in analogy with the nonrelativistic representation in Fig. 3.

The orbital eigenvalues obtained in the Dirac-Hartree-Fock procedure are—within order α^2—identical to the corresponding eigenvalues of the PHF operator (43),(46). Therefore, we shall study this operator further and, in particular, its relation to the nonrelativistic Hartree-Fock operator (8).

The effective spin-orbit interaction (45) is of order α^2, and hence, in this order, we can replace the relativistic orbitals by nonrelativistic ones

$$h'^{\,\mathrm{eff}}_{\mathrm{so}}(1)=V_1+\sum_a^{\mathrm{core}}(a\,|\,(V'_{12}+V'_{21})(1-P_{12})\,|\,a)_2\ . \tag{47}$$

This is identical to the nonrelativistic spin-orbit operator (23), apart from the fact that only the spin-own-orbit is considered.

We can now see that the difference between the Pauli-Hartree-Fock operator (46) and the nonrelativistic Hartree-Fock operator (8) has two sources. Firstly, it is the appearance of the effective spin-orbit operator, which gives rise to the first-order nonrelativistic (Hartree-Fock) fine-structure splittings. Secondly, it is the difference between the Hartree-Fock potentials of the two operators. We shall now demonstrate that the latter effect is completely equivalent to the nonrelativistic core polarization.

Let us define a new operator v as the difference between the PHF (44) and NRHF (7) potentials

$$\begin{aligned} v_1&=U_P^{\mathrm{HF}}(1)-U_S^{\mathrm{HF}}(1)\\ &=\sum_a^{\mathrm{core}}\left[\left[a_P\left|\frac{1}{r_{12}}(1-P_{12})\right|a_P\right]_2\right.\\ &\quad\left.-\left[a\left|\frac{1}{r_{12}}(1-P_{12})\right|a\right]_2\right]\ . \end{aligned} \tag{48}$$

FIG. 8. Graphical representation of the difference (48) between the Pauli-Hartree-Fock and the nonrelativistic Hartree-Fock potentials.

We can then express the PHF operator (46) as follows:

$$h_P^{\mathrm{HF}}(1)=h_S^{\mathrm{HF}}(1)+v_1+h'^{\,\mathrm{eff}}_{\mathrm{so}}(1)\ , \tag{49}$$

where

$$h_S^{\mathrm{HF}}(1)=h_S(1)+U_S^{\mathrm{HF}}(1) \tag{50}$$

is the nonrelativistic Hartree-Fock operator (8). The graphical representation of the potential difference (48) is given in Fig. 8, using the notations introduced in Fig. 7.

The nonrelativistic Hartree-Fock orbitals are eigenfunctions of the NRHF operator (50), and the corresponding relativistic orbitals in the Pauli scheme are eigenfunctions of the PHF operator (49). Thus, to order α^2 we can obtain the difference between the orbital eigenvalues of the two schemes using first-order perturbation theory

$$\Delta\epsilon=\langle m\,|\,h'^{\,\mathrm{eff}}_{\mathrm{so}}+v\,|\,m\rangle\ . \tag{51}$$

In order to find the effect of the potential difference v we have to consider the relativistic effect on the core orbitals. Again, using first-order perturbation theory, we can expand an arbitrary Pauli orbital as follows:

$$|\,j_P\rangle=|\,j\rangle+\sum_i^{i\neq j}\frac{|\,i\rangle\langle i\,|\,h'^{\,\mathrm{eff}}_{\mathrm{so}}+v\,|\,j\rangle}{\epsilon_j-\epsilon_i}\ . \tag{52}$$

This relation is shown graphically in Fig. 9. Inserting this expansion into the diagrams in Fig. 8, we get the relation in Fig. 10. It should be noted that the internal heavy lines in Fig. 8 do in fact represent *two* orbital lines which are joined. Each

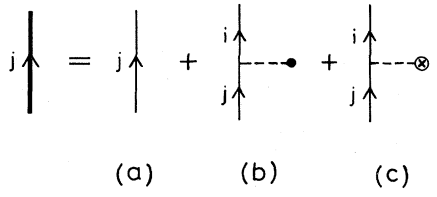

FIG. 9. Graphical representation of the expansion of the relativistic Hartree-Fock orbital in the Pauli approximation. Diagram (b) represents the contribution due to the effective spin-orbit interaction (47) and (c) the contribution due to the potential difference (48).

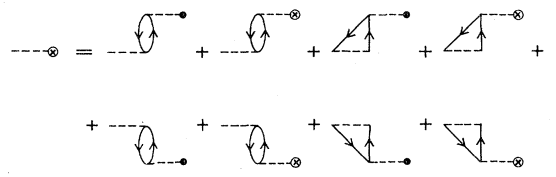

FIG. 10. Graphical form of the potential difference in Fig. 8, using the expansion of the relativistic orbitals in Fig. 9.

of them has to be replaced by the expansion in Fig. 9, which gives rise to diagrams pointing upwards as well as downwards, as shown in Fig. 10.

The potential difference v appears also on the right-hand side of the equation in Fig. 10, which implies that this equation has to be solved self-consistently. As mentioned previously, all diagrams vanish, if the effective spin-orbit interaction is connected to a closed orbital loop. The relation in Fig. 10 will therefore give rise to the expansion in Fig. 11, which contains exchange diagrams only.

It should be noted that the "folded" diagrams of the type (d),(e) and (h),(i), come out directly in factorized form, i.e., with the energy denominator equal to the product of the single excitation energies involved. Therefore, in the Goldstone representation[15–17] this corresponds to all possible time orderings between the interactions, exactly as in the polarization (or RPA) diagrams in Fig. 6.

Finally, we can now obtain the complete graphical representation of the eigenvalue difference (51) by means of the expansion in Fig. 11 and the representation of the effective spin-orbit interaction given in Fig. 3. Then we find that this is identical to the nonrelativistic core-polarized result—to all orders in the Coulomb interaction—exhibited in Fig. 6, provided, of course, that only the spin-own interaction is considered.

One important observation should be made here. We have assumed above that the core orbitals are generated in the relativistic Hartree-Fock potential

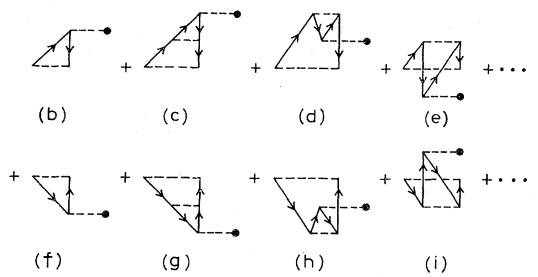

FIG. 11. Series expansion of the implicit equation represented in Fig. 10.

of the core, which in the Pauli approximation gives rise to the expansion in Fig. 9. The self-consistent treatment of the core orbitals is reflected by the fact that the potential difference v appears also on the right-hand side of the graphical equation in Fig. 10, which gives rise to the higher-order polarization diagrams in Fig. 11. In the calculations of Luc-Koenig,[6,7] the core orbitals are generated in a *local* potential, which means that the core exchange is not treated self-consistently. Then, her procedure cannot give rise to effects corresponding to the second- and higher-order core-polarization diagrams, i.e., diagrams (c)—(e) and (g)—(i) in Fig. 11.

V. NUMERICAL RESULTS FOR THE *nd* STATES OF SODIUMLIKE SYSTEMS

In order to illustrate the equivalence established above of the nonrelativistic many-body and the relativistic central-field approaches in evaluating the fine-structure separation, we shall consider the *nd* states of sodiumlike systems, which have been extensively studied experimentally as well as theoretically.[1–7] In recent years experimental data have been accumulated also for highly ionized systems of this sequence. (See, for example, the analysis by Edlén.[27]) Luc-Koenig[7] has very recently performed relativistic calculations for the $3d$ and $4d$ states of the sodium sequence up to $Z=50$, and we have made a similar extension of our many-body calculations. The results are summarized in Table I.

The first two columns of the table give the nonrelativistic first-order Hartree-Fock results, with and without the spin-other-orbit interaction, respectively, and the next two columns give the corresponding values when the core polarization is included to all orders. It is interesting to note that for the *nd* states of sodium the effect of the spin-other-orbit interaction is almost completely eliminated, when the core polarization is taken into account. This cancellation is accidental, of course, and does not occur for the heavier elements. The relativistic results of Luc-Koenig are given in the two following columns in Table I, with and without the exchange with the core in the potential for the valence electron. The significance of this difference will be discussed below.

The overall agreement between the theoretical and experimental results is quite good. This is illustrated in Fig. 12. In particular, it is observed that the transition from inverted to normal fine

TABLE I. Fine-structure separations (in cm^{-1}) for some *nd* states in the sodium isoelectronic sequence obtained in nonrelativistic many-body and relativistic central-field calculations.

		Hartree-Fock		Core polarization		Luc-Koenig		Expt.
		With soo	Without soo	With soo	Without soo	With exchange	Without exchange	
Na	3*d*	0.0335	0.0391	−0.0449	−0.0450	−0.05316	−0.04025	−0.0508
	4*d*	0.0137	0.0170	−0.0316	−0.0316	−0.03620	−0.02845	−0.0343
	5*d*	0.0069	0.0088	−0.0192	−0.0191			−0.0207
	6*d*	0.0040	0.0052	−0.0121	−0.0121			−0.0129
Mg^+	3*d*	0.580	0.784	−0.933	−0.825	−0.9931	−0.6505	−0.87
	4*d*	0.247	0.365	−0.572	−0.505	−0.6028	−0.4088	−0.52
	5*d*	0.127	0.195	−0.329	−0.290			
	6*d*	0.074	0.115	−0.201	−0.177			
Al^{2+}	3*d*	3.458	4.746	−2.961	−2.036	−3.445	−1.760	−2.29
	4*d*	1.552	2.265	−1.629	−1.097	−0.7094	−1.026	−1.19
Si^{3+}	3*d*	12.35	16.48	−3.322	+ .004	−4.463	−0.4283	−1.19
	4*d*	5.67	7.84	−1.420	+ 0.387	−1.931	−0.1937	− 0.12
P^{4+}	3*d*	32.43	41.86	+ 3.092	+ 11.15	+ 1.090	+ 8.273	+ 7.05
	4*d*	14.89	19.59	+ 2.736	+ 6.866	+ 1.885	+ 4.514	+ 5.13
S^{5+}	3*d*	70.54	88.46	+ 22.53	+ 38.17	+ 19.23	+ 30.06	+ 32
Cl^{6+}	3*d*	131.2	160.4	+ 61.90	+ 88.42	+ 56.99	+ 71.79	+ 73
K^{8+}	3*d*	353.6	416.6	+ 231.6	+ 291.2	+ 222.8	+ 246.3	+ 255
Ti^{11+}	3*d*	1076.8	1223.7	+ 849.7	+ 992.9			
Ni^{17+}	3*d*	5083	5554	+ 4543	+ 5011			
Mo^{28+}	3*d*	46010	48450	+ 44100	+ 46540	+ 44110	+ 44320	+ 44900

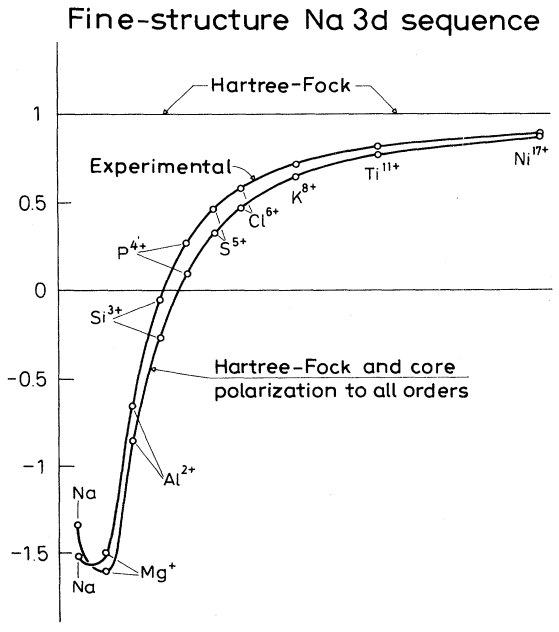

FIG. 12. Comparison between theoretical and experimental results for the fine structure of the Na 3*d* sequence.

structure occurs at the right place, namely, around Si.

Also the agreement between our many-body results and the central-field results of Luc-Koenig is satisfactory. As mentioned, however, the two calculations are not completely equivalent—not even to order α^2—due to the fact that the values of Luc-Koenig are obtained with a local potential for the core, while our many-body results correspond to relativistic results with the Hartree-Fock core potential. Therefore, in order to be able to make more accurate comparisons between the two approaches, we have performed calculations similar to those of Luc-Koenig, by means of our relativistic Hartree-Fock program.[26] The equation for the valence electron is then solved in the Hartree-Fock potential—with exchange—from the core. In principal, the fine structure will then appear directly as the eigenvalue difference. As mentioned previously, however, it is difficult to determine the eigenvalues with sufficient accuracy, and, therefore, following Luc-Koenig, we treat the exchange interaction as a perturbation.

The relativistic exchange interaction between an

TABLE II. Relativistic Hartree-Fock exchange integrals for the $3d$ states in sodium (in hartrees).

$G^1(2p_{1/2},3d_{3/2})=0.000\,140\,07$
$G^3(2p_{1/2},3d_{5/2})=0.000\,077\,11$
$G^1(2p_{3/2},3d_{3/2})=0.000\,141\,56$
$G^3(2p_{3/2},3d_{3/2})=0.000\,077\,89$
$G^1(2p_{3/2},3d_{5/2})=0.000\,141\,66$
$G^3(2p_{3/2},3d_{5/2})=0.000\,077\,95$

electron in the state (nlj) and a filled subshell $(n'l'j')$ is

$$-(2j'+1)\sum_k \begin{pmatrix} j' & k & j \\ \frac{1}{2} & 0 & -\frac{1}{2} \end{pmatrix}^2 G^k(n'l'j',nlj)\,, \tag{53}$$

where G^k is a radial exchange integral of Slater type. For sodiumlike systems only the $2p$ shell has to be considered, which leads to the following expressions for the two nd states:

$$\begin{aligned} &nd_{3/2}: \\ &-\tfrac{1}{3}G^1(2p_{1/2}nd_{3/2})-\tfrac{1}{15}G^1(2p_{3/2},nd_{3/2}) \\ &-\tfrac{9}{35}G^3(2p_{3/2},nd_{3/2})\,, \\ &nd_{5/2}: \\ &-\tfrac{1}{7}G^3(2p_{1/2},nd_{5/2})-\tfrac{2}{5}G^1(2p_{3/2},nd_{5/2}) \\ &-\tfrac{4}{35}G^3(2p_{3/2},nd_{5/2})\,. \end{aligned} \tag{54}$$

The exchange integrals for $3d$ state in Na are given in Table II, and in the first column (A) of Table III we give the difference in exchange for the two j states for systems with $Z=11-15$.

We know from the analysis made in the preceding section that the relativistic exchange gives rise to the core polarization, when we transform it into the nonrelativistic framework. The difference between the exchange expressions above, however, does not exactly correspond to the nonrelativistic core polarization given in Table I, as the following analysis will show.

In the Pauli approximation the exchange interaction is given by the exchange part of the PHF operator (43)

$$\sum_a^{\text{core}} \left(a_P \left| -P_{12}\left[\frac{1}{r_{12}}+V'_{12}+V'_{21}\right] \right| a_P \right)_2 \tag{55}$$

which we can represent graphically as in Fig. 13, where, as before, the heavy lines represent two-component Pauli spinors (large component). Diagram (a) represents the Coulomb part and diagram (b) the spin-(own-) orbit part. Expanding the orbitals in the same manner as in Figs. 9–11, we obtain the expansion given in Fig. 14.

Diagram (a) in Fig. 14 represents the nonrelativistic exchange integral which is j independent and hence cancels when we form the difference be-

TABLE III. The exchange polarization effect obtained in relativistic central-field and nonrelativistic many-body calculations (in cm^{-1}). The results in column B are corrected for the relativistic effect on the valence orbital, as described in the text.

		Relativistic Hartree-Fock		Nonrelativistic	Luc-	Pyper and
		A	*B*	many-body	Koenig	Marketos
Na	$3d$	−0.0950	−0.0820	−0.0841	−0.0750	−0.0685
	$4d$	−0.0546	−0.0473	−0.0486		−0.0389
	$5d$	−0.0308	−0.0272	−0.0280		−0.0222
	$6d$	−0.0178	−0.0167	−0.0172		−0.0135
Mg^+	$3d$	−1.855	−1.531	−1.610		
	$4d$	−1.000	−0.824	−0.870		
	$5d$	−0.542	−0.458	−0.485		
	$6d$	−0.304	−0.276	−0.292		
Al^{2+}	$3d$	−7.56	−6.28	−6.78		
	$4d$	−3.69	−3.08	−3.36		
Si^{3+}	$3d$	−17.3	−14.8	−16.48		
	$4d$	−7.5	−6.58	−7.46		
P^{4+}	$3d$	−30.0	−26.9	−30.72		
	$4d$	−11.8	−10.8	−12.72		

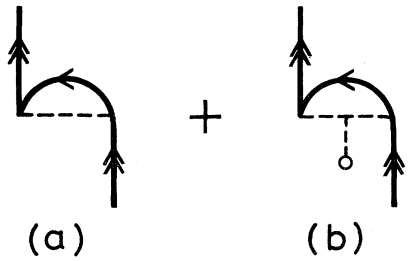

FIG. 13. Graphical representation of the relativistic exchange interaction (55).

tween the two j states. Diagram (b) represents the exchange part of the effective spin-own-orbit interaction (45) and diagrams (d),(f),... represent the core polarization. All these effects are included in the nonrelativistic many-body calculation. The remaining diagrams (c),(e), however, represent the effect on the exchange due to a relativistic correction to the *valence* orbital, which does *not* appear in the nonrelativistic core polarization. This effect is exactly canceled by the corresponding corrections to the direct Coulomb interaction and to the Schrödinger operator h_S due to the fact that the Hartree-Fock potential is used. Therefore, in order to make a correct, relativistic estimate—to order α^2—of the core polarization to be compared with the nonrelativistic results, we have to eliminate the effect due to the relativistic modification of the valence orbital from the exchange differences (54). Replacing the relativistic valence orbitals by the nonrelativistic nd orbital, this difference becomes

$$\tfrac{1}{3}[G^1(2p_{1/2},nd)-G^1(2p_{3/2},nd)] -\tfrac{1}{7}[G^3(2p_{1/2},nd)-G^3(2p_{3/2},nd)] . \quad (56)$$

For the values of the integrals given in Table II, we see that each square bracket above represents the difference between two numbers of approximately equal size. For that reason it is important that the same d orbital is used in each bracket. However, by replacing the nonrelativistic orbital in the first bracket by $nd_{3/2}$ and in the second by $nd_{5/2}$, very small errors are introduced. In this way we can estimate the expression (54) directly using the values in Table II, and the result is given in the second column (B) of Table III. In the third column of the same table we give the corresponding nonrelativistic core polarization, taken from Table I (without spin-other-orbit interaction). From the numerical comparison in Table III we see clearly the equivalence between the nonrelativistic core polarization and the relativistic exchange difference after corrections have been made for the relativistic contribution to the valence orbital, as described above. It is observed that the correction of the exchange integrals for the relativistic effect on the valence orbital—which is of order α^2—is quite important and improves the agreement significantly for the lighter elements. For the heavier elements the agreement is less good, which is most likely due to increased importance of α^4 contributions.

The fourth and fifth columns of Table III give the core-polarization contribution deduced by Luc-Koenig[7] and by Pyper and Marketos[11] from their relativistic calculations. For the $3d$ state of Na, Luc-Koenig has obtained the value -0.750 cm^{-1} for the core polarization, which is about 10% smaller than our results. This discrepancy is most likely due to the fact that Luc-Koenig uses a local potential, which implies that her results do not include higher-order perturbations, as demonstrated above. The core-polarization values obtained by Pyper and Marketos for the Na d states are about 20% smaller than our results. Although higher-order core-polarization contributions are included due to the use of HF core orbitals, the use of a hydrogenlike valence orbital underestimates the core-valence exchange interaction, since it fails to give a good description of the valence electron inside the core.

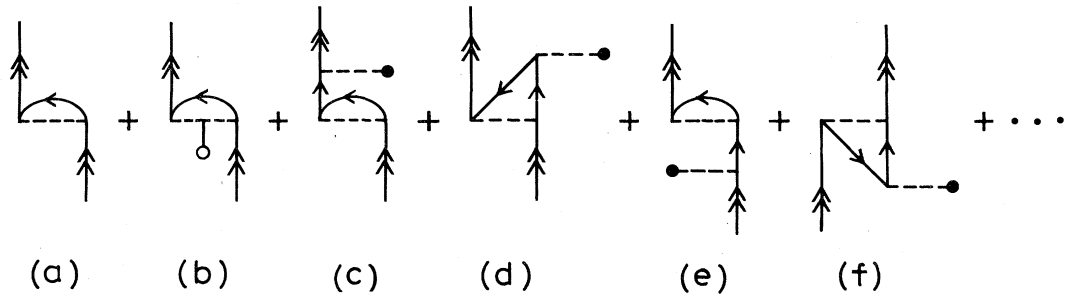

FIG. 14. Expansion of the relativistic diagrams in Fig. 13.

From our relativistic Hartree-Fock results of the core polarization given in Table III (column B) we can obtain corresponding values of the fine-structure splitting by adding the nonrelativistic Hartree-Fock results (without spin-other-orbit interaction), given in Table I. In order to include the effect of the spin-other-orbit interaction, we add the contribution obtained in our nonrelativistic core-polarization calculation. The result is shown for the first few elements of the sequence in the first column of Table IV, where we for convenience repeat our many-body results as well as the results of Luc-Koenig and the experimental values given in Table I. We give also the results of Pyper and Marketos.

Again we find that the agreement between our relativistic Hartree-Fock and nonrelativistic many-body results is quite good for the lighter elements, where the α^4 contributions should be quite small. Generally, our relativistic values agree better with the experimental results than do our many-body values. This is, of course, not surprising, considering the fact that the former contain certain contributions beyond α^2—in addition to the α^2 contributions, which are the same in the two approaches.

Some comments should be made about the two sets of values given by Luc-Koenig, with and without exchange from the core in the potential of the valence electron. As far as we can see, the only difference between the two calculations is that the exchange interaction between the valence electron and the core is included in a self-consistent way in the first case and to first order only in the second case. Since this exchange interaction is so weak, however, we find the difference surprisingly large. It should be noted that the core orbitals are generated in a local potential in both cases. Therefore, the arguments given above that the higher-order core-polarization effects are not included, hold for both sets of values. In our relativistic calculations the full Hartree-Fock potential is used within the core as well as between the core and the valence electron. Therefore, our relativistic results should be more equivalent to the values of Luc-Koenig *with* exchange, but again, due to the difference in the core potential, any closer comparison is not meaningful.

In comparing the final results of Pyper and Marketos it should be borne in mind that, whereas they have included the core-valence contribution from the spin-other-orbit interaction, they have neglected the correction to the core-valence exchange interaction due to the effect of the spin-other-orbit operator on the core orbitals. As we have seen in Table I, the effect of the spin-other-orbit operator on the core polarization essentially cancels the effect on the valence electrons for the Na d states.

As far as a comparison with experiment is concerned, however, it is found that all sets of values given in Table IV give essentially the same kind of agreement, indicating that the discrepancies can well be explained by the approximations discussed here. In particular, it seems that the effect of electron correlation—i.e., due to multiple excitations—is relatively small for the sodium sequence.

TABLE IV. Comparison between theoretical and experimental values for the fine-structure separation (in cm^{-1}).

		Present work		Luc-Koenig			
		Relativ. HF	Nonrel. many-body	With exchange	Without exchange	Pyper and Marketos	Expt.
Na	3*d*	−0.0428	−0.0449	−0.0532	−0.0402	−0.0359	−0.0508
	4*d*	−0.0303	−0.0316	−0.0362	−0.0284	−0.0258	−0.0343
Mg^+	3*d*	−0.855	−0.933	−0.993	−0.650		−0.87
	4*d*	−0.526	−0.572	−0.603	−0.409		−0.52
Al^{2+}	3*d*	−2.45	−2.96	−3.44	−1.76		−2.29
	4*d*	−1.35	−1.63	−0.71	−1.03		−1.19
Si^{3+}	3*d*	−1.64	−3.32	−4.46	−0.43		−1.19
	4*d*	−0.54	−1.42	−1.93	−0.19		−0.12
P^{4+}	3*d*	+6.9	+3.09	+1.09	+8.27		+7.05
	4*d*	+4.7	+2.74	+1.88	+4.51		+5.13

This might be somewhat surprising in view of the fact that such effects have been found to be highly important for the hyperfine interaction in many cases.[13] In applying the technique demonstrated here to the fine structure of heavier alkali-metal elements, however, we find that nonrelativistic core polarization is not sufficient in order to obtain agreement with experiments. This is illustrated by means of the results for the $4d$ state in Rb, given in Table V. Here it is found that the residual discrepancy between theory and experiment is comparable to the effect of core polarization. Whether this is primarily due to correlation effects or to effects beyond α^2, cannot be said at present.

VI. SUMMARY AND CONCLUSIONS

Using the Pauli approximation and the graphical representation of Goldstone type, we have shown in detail that for alkali-metal-like systems the relativistic Hartree-Fock (Dirac-Fock) procedure—based on a many-body Dirac Hamiltonian without Breit interactions—is to order α^2 equivalent to a nonrelativistic many-body calculation, where the core polarization due to combined spin-orbit (without spin-other-orbit) and Coulomb interactions are taken into account to first order in the spin-orbit interaction and to all orders in the Coulomb interaction.

The difference between the relativistic and nonrelativistic Hartree-Fock procedures has mainly two sources; firstly, the effective spin-orbit interaction, which originates from the elimination of the small component of the relativistic wave function, and, secondly, the difference between the relativistic and the nonrelativistic Harteee-Fock potentials.

TABLE V. Theoretical and experimental fine-structure separations (in cm^{-1}) for the $4d$ state in Rb (from Ref. 5).

	Present work		
	With soo	Without soo	Lee *et al.*[a]
Nonrelativistic Hartree-Fock	12.91	13.67	13.23
With polarization	−11.80	−11.41	−10.22
Experimental	−0.44		

[a]Reference 2.

The effective spin-orbit interaction yields essentially the nonrelativistic, first-order (Hartree-Fock) contribution to the fine-structure splitting, which is always positive. The difference between the Hartree-Fock potentials, on the other hand, corresponds to a nonrelativistic core polarization, which yields a negative contribution, in some cases large enough to cause a fine-structure inversion. The Hartree-Fock potential used in the present analysis depends only on the core orbitals, and therefore it follows that the potential difference is due solely to relativistic effects on the core. The corresponding effect on the valence orbital does not affect the fine structure in order α^2. This agrees with the interpretation recently given by Luc-Koenig,[7] but it disagrees with the interpretation given earlier.[6]

The equivalence on the relativistic and nonrelativistic approaches is demonstrated numerically by comparing our many-body results with relativistic Hartree-Fock calculations. The results of Luc-Koenig, being based on a local core potential, are only partially equivalent to our many-body results.

From the comparison between the relativistic and nonrelativistic results, we can draw the conclusion that α^4 and higher-order contributions are comparatively small at the beginning of the sequence but become significant for the heavier elements. From the comparison between the theoretical and experimental results, furthermore, we can draw the conclusion that the correlational effects—due to multiple excitations—are comparatively small. Therefore, in order to achieve higher accuracy of the fine-structure separations of this sequence, it would be of interest to evaluate the polarization effects in a relativistic way, which would correspond to including important α^4 contribu-

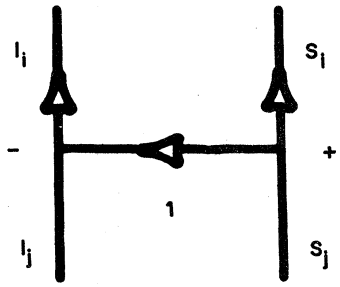

FIG. 15. Angular-momentum graph representing $G1$. In the graphs, each vertex represents a 3-j symbol and the sign at the vertex tells if the angular momenta are taken in positive or negative direction. An arrow on an lm line carries a phase factor $(-1)^{l-m}$ and charges the sign of m. Summation over m values of internal lines is implied.

tions. Such calculations would be feasible with the programs that are now available or are being developed.[28] For other systems—like the Rb atom discussed above—it seems that correlational effects could be of great importance. Such effects can be calculated with a technique similar to that used for the hyperfine structure.[12,13,17]

The authors acknowledge the discussions with Professor Bengt Edlén concerning the experimental aspects and with Sten Salomonson concerning the theoretical aspects of this work.

APPENDIX

The matrix elements in (22) of the effective one-body spin-orbit interaction will here be expressed as

$$\langle i \mid h_{\rm so}^{\rm eff} \mid j \rangle = \rho(i,j) \langle i \mid \vec{l} \cdot \vec{s} \mid j \rangle ,$$

where

$$\langle i \mid \vec{l} \cdot \vec{s} \mid j \rangle = \langle l_i \mid \vec{l} \mid l_j \rangle \langle s_i \mid \vec{s} \mid s_j \rangle (-G_1)$$

and

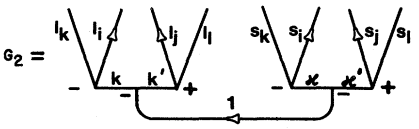

FIG. 16. Angular part of the matrix element of the two-body operator.

$$G_1 = \sum_q (-1)^{1-q+l_i-m_i+s_i-m_{si}} \begin{pmatrix} l_i & 1 & l_j \\ -m_i & q & m_j \end{pmatrix} \begin{pmatrix} s_i & 1 & s_j \\ -m_{si} & -q & m_{sj} \end{pmatrix}$$

is the angular part, which can be represented by the angular-momentum graph in Fig. 15.

The contribution to $\rho(i,j)$ from the one-body operator V_1 in (19) is simply given by

$$\rho_1(i,j) = \frac{\alpha^2}{2} Z \left\langle n_i l_i \left| \frac{1}{r^3} \right| n_j l_j \right\rangle . \tag{A1}$$

The two-body operator (20) is more complicated. It can be written in a more convenient tensor form

$$\begin{aligned} V_{ij} = \frac{\alpha^2}{2} \sum_k \frac{(-1)^k}{\sqrt{3}} \Bigg[& \frac{r_j^k}{r_i^{k+3}} \epsilon(r_i - r_j)(2k+1)(2k+3)^{1/2} [(\vec{C}^k \vec{l})_i^{k+1} \vec{C}_j^k]^1 - \frac{r_i^{k-2}}{r_j^{k+1}} \epsilon(r_j - r_i)(2k+1)(2k-1)^{1/2} \\ & \times [(\vec{C}^k \vec{l})_i^{k-1} \vec{C}_j^k]^1 - \left[\frac{r_i^{k-2}}{r_j^{k+1}} \epsilon(r_j - r_i)(k+1) - \frac{r_j^k}{r_i^{k+3}} \epsilon(r_i - r_j) \cdot k \right] (2k+1)^{1/2} [(\vec{C}^k \vec{l})_i^k \vec{C}_j^k]^1 \\ & + r_j \frac{r_<^{k-1}}{r_>^{k+2}} \frac{\partial}{\partial r_i} [k(k+1)(2k+1)]^{1/2} (\vec{C}_i^k \vec{C}_j^k)^1 \Bigg] \cdot (\vec{s}_i + 2\vec{s}_j) , \end{aligned} \tag{A2}$$

where $\epsilon(X)$ is the step function which is 1 for $X > 0$ and 0 for $X < 0$.

All the operators in V_{12} can be written in the general form

$$U = f(r_1, r_2) [\vec{U}^k(1) \vec{U}^{k'}(2)]^1 \cdot [\vec{s}^{\kappa}(1) \vec{s}^{\kappa'}(2)]^1 .$$

A general matrix element of an operator of this type can be written as

$$\begin{aligned} \langle ij \mid U \mid kl \rangle = & \sum_{q m m' m_s m_s'} (-1)^q \langle kk' m m' \mid kk' l q \rangle \langle \kappa \kappa' m_s m_s' \mid \kappa \kappa' 1 - q \rangle \\ & \times \langle ij \mid f(r_1, r_2) \vec{U}_m^k(1) \vec{U}_{m'}^{k'}(2) \vec{s}_{m_s}^{\kappa}(1) \vec{s}_{m_s}^{\kappa'}(2) \mid kl \rangle \\ = & 3(-1)^{k'-k+\kappa'-\kappa} \langle n_i l_i, n_j l_j \mid f(r_1, r_2) \mid n_k l_k, n_l l_l \rangle \langle l_i \| \vec{U}^k \| l_k \rangle \langle l_j \| \vec{U}^{k'} \| l_l \rangle \\ & \times \langle s_i \| \vec{s}^{\kappa} \| s_k \rangle \langle s_j \| \vec{s}^{\kappa'} \| s_l \rangle (-G_2) , \end{aligned} \tag{A3}$$

where G_2 has the analytical expression

$$G_2=\sum_{qmm'm_sm_s'}(-1)^{1-q+1_i-m_i+l_j-m_j+s_i-m_{si}+s_j-m_{sj}}\begin{pmatrix} l_i & k & l_k \\ -m_i & m & m_k\end{pmatrix}\begin{pmatrix} l_j & k' & l_i \\ -m_j & m' & m_l\end{pmatrix}\begin{pmatrix} s_i & \kappa & s_k \\ -m_{si} & m_s & m_{sk}\end{pmatrix}$$
$$\times\begin{pmatrix} s_j & \kappa' & s_l \\ -m_{sj} & m_s' & m_{sl}\end{pmatrix}\begin{pmatrix} k & k' & 1 \\ m & m' & q\end{pmatrix}\begin{pmatrix} \kappa & \kappa' & 1 \\ m_s & m_s' & -q\end{pmatrix}$$

and is represented by the angular-momentum graph in Fig. 16.

Only the direct and exchange matrix elements are needed in (20). The direct matrix element of U is

$$\sum_b^{\text{occ}}\langle ib\mid U\mid jb\rangle=3(-1)^{k'-k+\kappa'-\kappa}\sum_{n_bl_b}\langle l_i||\vec{U}^k||l_j\rangle\langle l_b||\vec{U}^{k'}||l_b\rangle\langle s_i||\vec{s}^{\kappa}||s_j\rangle\langle s_b||\vec{s}^{\kappa'}||s_b\rangle$$
$$\times\langle n_il_i,n_bl_b\mid f(r_1,r_2)\mid n_jl_j,n_bl_b\rangle(-G_d)\ ,$$

where G_d is shown in Fig. 17. The summations over m_b and m_{sb} have been performed by joining in G_2 the two l_b and s_b lines, respectively. Using the rules for angular momentum graphs, G_d can be reduced giving

$$G_d=\tfrac{1}{3}\sqrt{2(2l_b+1)}\delta(\kappa',0)\delta(\kappa,1)\delta(k',0)\delta(k,1)G_1$$
$$=-\tfrac{1}{3}\sqrt{2(2l_b+1)}\delta(\kappa',0)\delta(\kappa,1)\delta(k',0)\delta(k,1)\frac{\langle i\mid\vec{l}\cdot\vec{s}\mid j\rangle}{\langle l_i||\vec{l}||l_j\rangle\langle s_i||\vec{s}||s_j\rangle}\ .$$

Only the first term in V_{12} satisfies the restrictions on the k values and the spin-other-orbit part, which has $\kappa'=1$, vanishes. The second term in V_{21} gives no contribution since

$$\langle l||(\vec{C}^1\vec{l})^0||l\rangle=0\ .$$

The relations

$$\langle l'||(\vec{C}^k\vec{l})^{k'}||l\rangle=\sqrt{2k'+1}(-1)^{k'-k}\begin{Bmatrix} k & 1 & k' \\ l & l' & l\end{Bmatrix}\langle l'||\vec{C}^k||l\rangle\langle l||\vec{l}||l\rangle$$

and

$$\begin{Bmatrix} 0 & 1 & 1 \\ l & l & l\end{Bmatrix}=\frac{-1}{\sqrt{3(2l+1)}}$$

give the direct matrix elements

$$\sum_b^{\text{occ}}\left\langle ib\left|-\frac{\alpha^2}{2}\frac{1}{r_{12}^3}(\vec{r}_{12}\times\vec{p}_1)\cdot(\vec{s}_1+2\vec{s}_2)\right|jb\right\rangle$$
$$=-\frac{\alpha^2}{2}\sum_{n_bl_b}\sqrt{2(2l_b+1)}N^0(i,b,j,b)\sqrt{3}(-1)\begin{Bmatrix} 0 & 1 & 1 \\ l_j & l_i & l_j\end{Bmatrix}\langle l_i||\vec{C}^0||l_j\rangle\langle l_b||\vec{C}^0||l_b\rangle\langle s||1||s\rangle\langle i\mid\vec{l}\cdot\vec{s}\mid j\rangle$$
$$=\zeta_d(i,j)\langle i\mid\vec{l}\cdot\vec{s}\mid j\rangle\ ,$$

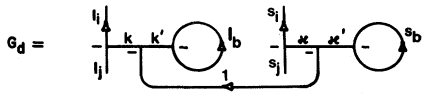

FIG. 17. Angular part of the direct matrix element.

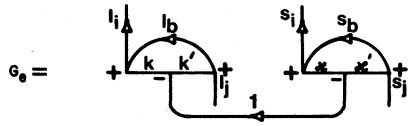

FIG. 18. Angular part of the exchange matrix element.

where

$$\zeta_d(i,j)=-\frac{\alpha^2}{2}\sum_{n_b l_b} 2(2l_b+1)N^0(i,b,j,b) \tag{A4}$$

and

$$N^k(i,j,k,l)=\int_0^\infty dr_1 P_i(r_i)P_k(r_l)\frac{1}{r_1^{k+3}}\int_0^{r_1} dr_2 P_j(r_2)P_l(r_2)r_2^k \ .$$

[Note that $N^k(i,j,k,l)\neq N^k(j,i,l,k)$ if $j\neq k$ or $i\neq l$.]

Applying the general expression (A3) on the exchange matrix element gives

$$\begin{aligned}\langle ib \mid U \mid bj\rangle =& 3(-1)^{k'-k+\kappa'-\kappa}\langle ib \mid f(r_1,r_2) \mid bj\rangle\langle l_i||\vec{\mathrm{U}}^k||l_b\rangle \\ &\times\langle l_b||\vec{\mathrm{U}}^{k'}||l_j\rangle\langle s_i||\vec{\mathrm{s}}^\kappa||s_b\rangle\langle s_b||\vec{\mathrm{s}}^{\kappa'}||s_j\rangle(-G_e)\ ,\end{aligned} \tag{A5}$$

where G_e is shown in Fig. 18 and can be reduced to

$$G_e=\begin{Bmatrix} l_i & l_j & 1 \\ k' & k & l_b \end{Bmatrix}\begin{Bmatrix} s_i & s_j & 1 \\ \kappa' & \kappa & s_b \end{Bmatrix}(-1)^{k+k'+\kappa+\kappa'}G_1(-1)^{l_i+l_j+1} \ .$$

The second $6j$ symbol always has the value $1/\sqrt{6}$ since either $\kappa'=0,\kappa=1$ or $\kappa'=1,\kappa=0$.

Using (A5) to evaluate the exchange matrix element of the first term in (A2) gives

$$\begin{aligned}&\frac{\alpha^2}{2}\sum_b^{\text{occ}}\left\langle ib\left|\sum_k \frac{(-1)^k}{\sqrt{3}}\frac{r_2^k}{r_1^{k+3}}\epsilon(r_1-r_2)(2k+1)(2k+3)^{1/2}[(\vec{\mathrm{C}}^k\vec{1})_1^{k+1}\vec{\mathrm{C}}_2^k]^1\cdot(\vec{\mathrm{s}}_1+2\vec{\mathrm{s}}_2)\right|b_j\right\rangle \\ &=\frac{3\alpha^2}{2}\sum_{n_b l_b}^{\text{occ}}\sum_k \frac{(-1)^k}{\sqrt{3}}N^k(i,b,b,j)(2k+1)(2k+3)(-1)\begin{Bmatrix} k & 1 & k+1 \\ l_b & l_i & l_b \end{Bmatrix} \\ &\quad\times\langle l_b||\vec{1}||l_b\rangle\langle l_i||\vec{\mathrm{C}}^k||l_b\rangle\langle l_b||\vec{\mathrm{C}}^k||l_j\rangle\cdot 3\langle s||\vec{\mathrm{s}}||s\rangle\langle s||1||s\rangle \\ &\quad\times\begin{Bmatrix} k & k+1 & 1 \\ l_i & l_j & l_b \end{Bmatrix}\cdot\frac{1}{\sqrt{6}}\frac{\langle i\mid\vec{1}\cdot\vec{\mathrm{s}}\mid j\rangle}{\langle s_i||\vec{\mathrm{s}}||s_j\rangle\langle l_i||\vec{1}||l_j\rangle}(-1)^{l_i+l_j+1} \\ &=\frac{3\alpha^2}{2}\sum_k(2k+1)(2k+3)\begin{Bmatrix} k & 1 & k+1 \\ l_b & l_i & l_b \end{Bmatrix}\begin{Bmatrix} k & k+1 & 1 \\ l_i & l_j & l_b \end{Bmatrix}X^k(l_i,l_b,l_b,l_j)N^k(i,b,b,j)\frac{\langle l_b||\vec{1}||l_b\rangle}{\langle l_i||\vec{1}||l_j\rangle}\langle i\mid\vec{1}\cdot\vec{\mathrm{s}}\mid j\rangle .\end{aligned}$$

The other terms in (A2) can be treated in the same way, giving

$$\begin{aligned}\zeta_e(i,j)=&\frac{3\alpha^2}{2}\delta(l_i,l_j)\sum_{n_b l_b}\sum_k X^k(l_i,l_b,l_b,l_j) \\ &\times\Bigg[(2k+1)(2k+3)\begin{Bmatrix} k+1 & k & 1 \\ l_i & l_i & l_b \end{Bmatrix} \\ &\quad\times\left[\begin{Bmatrix} k+1 & k & 1 \\ l_b & l_b & l_i \end{Bmatrix}\frac{\langle l_b||\vec{1}||l_b\rangle}{\langle l_i||\vec{1}||l_i\rangle}N^k(i,b,b,j)+\begin{Bmatrix} k+1 & k & 1 \\ l_i & l_i & l_b \end{Bmatrix}N^k(b,i,j,b)\right] \\ &\quad-(2k+1)(2k-1)\begin{Bmatrix} k-1 & k & 1 \\ l_i & l_i & l_b \end{Bmatrix} \\ &\quad\times\left[\begin{Bmatrix} k-1 & k & 1 \\ l_b & l_b & l_i \end{Bmatrix}\frac{\langle l_b||\vec{1}||l_b\rangle}{\langle l_i||\vec{1}||l_i\rangle}N^{k-2}(b,i,j,b)\begin{Bmatrix} k-1 & k & 1 \\ l_i & l_i & l_b \end{Bmatrix}N^{k-2}(i,b,b,j)\right]\end{aligned}$$

$$+(2k+1)\begin{Bmatrix} k & k & 1 \\ l_i & l_i & l_b \end{Bmatrix}\left[\begin{Bmatrix} k & k & 1 \\ l_b & l_b & l_i \end{Bmatrix}\frac{\langle l_b||\vec{1}||l_b\rangle}{\langle l_i||\vec{1}||l_i\rangle}[(k+1)N^{k-2}(b,i,j,b)-kN^k(i,b,b,j)]\right.$$

$$\left.-\begin{Bmatrix} k & k & 1 \\ l_i & l_i & l_b \end{Bmatrix}[(k+1)N^{k-2}(i,b,b,j)-kN^k(b,i,j,b)]\right]$$

$$+\frac{1}{\langle l_i||\vec{1}||l_i\rangle}[k(k+1)(2k+1)]^{1/2}\begin{Bmatrix} k & k & 1 \\ l_i & l_i & l_b \end{Bmatrix}[V^{k-1}(b,i,j,b)-V^{k-1}(i,b,b,j)]\Bigg] . \tag{A6}$$

All the matrix elements are now in the desired form (24) and the parameter $\rho(i,j)$ is obtained by combining Eqs. (A1), (A4), and (A6) using

$$\rho(i,j)=\rho_1(i,j)+\rho_d(i,j)+\rho_e(i,j) .$$

---

[1]C. E. Moore, *Atomic Energy Levels,* Natl. Bur. Stds. (U.S. GPO, Washington, D.C., 1971).

[2]H. M. Foley and R. M. Sternheimer, Phys. Lett. 55A, 276 (1975); T. Lee, J. E. Rogers, T. P. Das, and R. M. Sternheimer, Phys. Rev. A 14, 51 (1976); R. M. Sternheimer, J. E. Rogers, T. Lee, and T. P. Das, *ibid.* 14, 1575 (1976)

[3]D. R. Beck and C. A. Nicolaides, in Proceedings of the Atomic Spectroscopy Symposium, National Bureau of Standards, Washington, D. C., 1975, p. 60 (unpublished).

[4]L. Holmgren, I. Lindgren, J. Morrison, and A. -M. Mårtensson, Z. Phys. A 276, 179 (1976).

[5]A. -M Mårtensson, thesis, University of Göteborg, 1978 (unpublished).

[6]E. Luc-Koenig, Phys. Rev. A 13, 2114 (1976).

[7]E. Luc-Koenig, J. Phys. (Paris) 41, 1273 (1980).

[8]G. E. Brown and D. G. Ravenhall, Proc. R. Soc. London, Ser. A 208, 552 (1951).

[9]J. Sucher, Phys. Rev. A 22, 348 (1980).

[10]M. H. Mittlemann, Phys. Rev. A 24, 1167 (1981).

[11]N. C. Pyper and P. Marketos, J. Phys. B 14, 4469 (1981).

[12]S. Garpman, I. Lindgren, J. Lindgren, and J. Morrison, Z. Phys. A 276, 167 (1976).

[13]I. Lindgren, J. Lindgren, and A. -M. Mårtensson, Z. Phys. A 279, 113 (1976); Phys. Rev. A 15, 2123 (1977).

[14]T. Koopmans, Physica (Utrecht) 1, 104 (1934).

[15]J. Goldstone, Proc. R. Soc. London, Ser. A 239, 267 (1957).

[16]H. P. Kelly, Adv. Chem. Phys. 14, 129 (1969).

[17]I. Lindgren and J. Morrison, *Atomic Many-Body Theory,* Vol. 13 of Springer Series in Chemical Physics (Springer, Heidelberg, 1982).

[18]H. A. Bethe and E. E. Salpeter, *Quantum Mechanics of One- and Two-Electron Atoms* (Springer, Berlin, 1957).

[19]A. L. Akhietzer and V. B. Berestetskii, *Quantum Electrodynamics* (Wiley Interscience, New York, 1965).

[20]L. Armstrong and S. Feneuille, *Advances in Atomic and Molecular Physics* (Academic, San Francisco, 1974), Vol. 10.

[21]M. Blume and R. E. Watson, Proc. R. Soc. London, Ser. A 270, 127 (1962); 271, 565 (1963).

[22]K. -N. Huang and A. F. Starace, Phys. Rev. A 10, 354 (1978).

[23]R. M. Sternheimer, Phys. Rev. 80, 102 (1950); 84, 244 (1951); 86, 316 (1952).

[24]D. J. Thouless, *The Quantum Mechanics of Many-Body Systems* (Academic, New York, 1972).

[25]I. P. Grant, Adv. Phys. 19, 747 (1970).

[26]I. Lindgren and A. Rosén, Case Stud. At. Phys. 4, 93 (1974).

[27]B. Edlén, Phys. Scr. 17, 564 (1978).

[28]J. -L. Heully, A. -M. Mårtensson, and S. Salomonson (private communication).